

UC Berkeley

UC Berkeley Previously Published Works

Title

Nox2 redox signaling maintains essential cell populations in the brain

Permalink

<https://escholarship.org/uc/item/40c551cs>

Journal

Nature Chemical Biology, 7(2)

ISSN

1552-4450

Authors

Dickinson, Bryan C
Peltier, Joseph
Stone, Daniel
[et al.](#)

Publication Date

2011-02-01

DOI

10.1038/nchembio.497

Peer reviewed



HHS Public Access

Author manuscript

Nat Chem Biol. Author manuscript; available in PMC 2011 August 01.

Published in final edited form as:

Nat Chem Biol. 2011 February ; 7(2): 106–112. doi:10.1038/nchembio.497.

Nox2 redox signaling maintains essential cell populations in the brain

Bryan C Dickinson¹, Joseph Peltier², Daniel Stone², David V Schaffer², and Christopher J Chang^{1,3}

¹Department of Chemistry, University of California, Berkeley, CA 94720

²Department of Chemical Engineering, University of California, Berkeley, CA 94720

³Howard Hughes Medical Institute, University of California, Berkeley, CA 94720

Abstract

Reactive oxygen species (ROS) are conventionally classified as toxic consequences of aerobic life, and the brain is particularly susceptible to ROS-induced oxidative stress and damage owing to its high energy and oxygen demands. In this context, NADPH oxidases (Nox) are a widespread source of brain ROS implicated in seizures, stroke, and neurodegeneration. A physiological role for ROS generation in normal brain function has not been established, despite the fact that mice and humans lacking functional Nox proteins exhibit cognitive deficits. Using molecular imaging with Peroxyfluor-6 (PF6), a new selective fluorescent indicator for hydrogen peroxide (H₂O₂), we show that adult hippocampal stem/progenitor cells (AHPs) generate H₂O₂ through Nox2 to regulate intracellular growth signaling pathways, which in turn maintains their normal proliferation *in vitro* and *in vivo*. Our results challenge the traditional view that brain ROS are solely deleterious by demonstrating that controlled ROS chemistry is needed for maintaining specific cell populations.

Aberrant accumulation of reactive oxygen species (ROS) over time can trigger oxidative stress and damage¹ of proteins, lipids, and nucleic acids that form the molecular underpinning of the free-radical theory of aging². The brain is particularly sensitive to ROS damage owing to its high oxygen demand and low antioxidant capacity, and oxidative stress is connected to stroke and neurodegenerative diseases where age is a risk factor³. However, this organ also purposefully produces ROS throughout development and adult life, and a major source of brain ROS are the NADPH oxidase enzymes (Nox) that are expressed throughout the central nervous system (CNS)^{4,5}. These membrane-spanning protein

Users may view, print, copy, download and text and data- mine the content in such documents, for the purposes of academic research, subject always to the full Conditions of use: http://www.nature.com/authors/editorial_policies/license.html#terms

Correspondence to: David V Schaffer; Christopher J Chang.

Author Contributions: B.C.D. synthesized all compounds in the paper, as well as performing all analytical measurements, imaging assays, and cell culture and mouse experiments. J.P. collaborated on cell culture, RT-PCR, and mouse experiments. D.S. helped with mouse experiments. C.J.C., D.V.S., B.C.D., and J.P. designed experimental strategies. C.J.C. and B.C.D. wrote the paper with input from all co-authors.

Competing financial interests: The authors declare no competing financial interests.

Additional Information: Full descriptions of all materials and methods can be found in the Supplementary Materials and Methods.

complexes generate hydrogen peroxide (H_2O_2) as their final chemical product by the direct two-electron reduction of molecular oxygen by NAPDH_{5,6}, or through the one-electron reduction to superoxide (O_2^-) followed by conversion to H_2O_2 ^{4,5}. The established physiological function for Nox proteins is in the immune system, where they participate in phagocytic killing of pathogen invaders⁵. More recently, however, the discovery of Nox enzymes in nonphagocytic cell types throughout the body^{6,7} has greatly expanded the scope and potential roles for these complexes, and emerging data links their H_2O_2 -producing activity to beneficial cell signaling events⁴⁻¹⁵.

The H_2O_2 generated from Nox proteins in the brain and CNS has been traditionally associated with stroke¹⁶, aging¹⁷, seizures¹⁸, and neurodegenerative Alzheimer's¹⁹ and Parkinson's²⁰ diseases. However, the presence of these proteins in the brain and CNS throughout adult life presages a beneficial role for endogenous ROS production that remains insufficiently understood²¹. Along these lines, both mice and humans that lack functional Nox2 exhibit cognitive deficits^{22,23}, most notably in learning and memory, suggesting a role for this Nox isoform within the hippocampus. In this context, a population of neural stem/progenitor cells reside within the dentate gyrus of the hippocampus and form new neural tissue in the adult brain that plays a role in memory formation²⁴. We hypothesized that Nox-generated H_2O_2 , which acts as a molecular signal for growth within cultured cell lines^{8,9}, could help maintain the proliferation of these stem cell populations in the brain.

In this report, we show that H_2O_2 redox signaling derived from Nox2 is essential for normal growth and proliferation of neural stem cells *in vitro* and *in vivo*. Motivated by the dearth of chemical tools to selectively probe H_2O_2 production in cell types that would not be expected to produce high concentrations of this ROS, we developed Peroxyfluor-6 acetoxymethyl ester (PF6-AM), a new chemoselective fluorescent indicator for H_2O_2 with improved sensitivity. This fluorescent probe features a boronate chemical switch that allows for selective detection of H_2O_2 over other ROS, combined with acetoxymethyl ester (AM) protected phenol and carboxylic acid groups for enhanced cellular retention and sensitivity. After validating that PF6 is more responsive than previous boronate H_2O_2 reporters, we use this new trappable probe to demonstrate that adult hippocampal stem/progenitor (AHP) cells produce H_2O_2 when stimulated with fibroblast growth factor 2 (FGF-2), a mitogen that regulates their proliferation²⁵. We then show that endogenous H_2O_2 production is important for normal cell signaling through the kinase hub Akt and is mediated by the H_2O_2 -producing enzyme Nox2. Moreover, RNAi knockdown of Nox2 in cell culture and gene knockout of Nox2 in mice abrogates normal Akt signaling and AHP function *in vitro* and *in vivo*. Our results highlight the utility of PF6-AM as a tool to help discover new redox chemistry in biological systems and provide evidence that the controlled production of H_2O_2 in the brain can be beneficial to its physiology.

Results

Synthesis and evaluation of Peroxyfluor-6 (PF6)

Redox signaling mediated by H_2O_2 has been studied primarily in proliferating cell culture models stimulated with mitogens⁹. As the majority of brain tissue is comprised of terminally differentiated cells, we turned our attention to AHPs, which grow and proliferate throughout

development and adult life to feed into neuronal and glial populations. Accordingly, we first sought to test whether these neural stem cells produce endogenous H₂O₂ under growth conditions. In this regard, traditional methodologies for imaging H₂O₂ and related ROS in living cells typically utilize non-specific indicators that rely on general oxidation and therefore detect an assortment of oxidants²⁶. Because neural tissue is highly susceptible to oxidative stress^{1,2,21,27} the specific ROS that the AHPs come in contact with is a critical determinant of the ultimate downstream cellular responses. We have shown that the conversion of aryl boronates to phenols is a useful chemoselective methodology for the detection of H₂O₂ in biological systems²⁸. The first generation of Peroxy dyes, exemplified by PF1 (Supplementary Fig. 1), possess two boronate protecting groups, which after reaction with two equivalents of H₂O₂, yield fluorescent products²⁹⁻³². This initial work established that boronate cages offer a general motif for creating fluorescent indicators that can selectively image H₂O₂ over other biologically relevant ROS. Second generation boronate probes such as PG1 and MitoPY1 (Supplementary Fig. 1) utilize a single boronate deprotection to increase sensitivity and allow for detection of H₂O₂ generated in oxidative stress³³, neurodegenerative disease^{34,35}, immune³⁶, and growth factor signaling models^{37,38}. Unfortunately, these available boronate dyes were not sufficiently sensitive to visualize potential H₂O₂ production in AHPs after stimulation with the endogenous mitogen FGF-2 (Supplementary Fig. 2).

We sought to improve the sensitivity of boronate-based probes while maintaining their high selectivity for H₂O₂. Inspired by work showing that increasing cellular retention of fluorescent probes is a practical strategy to improve sensitivity³⁹⁻⁴³, we designed and synthesized PF6-AM, a carboxyfluorescein-based probe combining a boronate-masked phenol for H₂O₂ detection and AM groups to cap phenol and carboxylic acid functionalities for enhanced cellular retention (Scheme 1). Briefly, monotriflation of 6-carboxyfluorescein using stoichiometric *N*-phenyl bis(trifluoromethanesulfonamide) affords triflate **2** in 60% yield. Palladium-mediated borylation of **2** with cyclohexyl JohnPhos, bis(pinacolato)diboron, and diisopropylethylamine in anhydrous 1,4-dioxane at room temperature provides PF6 in 80% yield. Finally, protection with bromomethyl acetate furnishes AM-ester protected PF6-AM. The lipophilic AM esters allow the probe to pass readily through cell membranes, where esterases can then deprotect the AM groups to reveal PF6, a dianionic form of the probe that is membrane impermeable and thus trapped inside the cell, where it can respond to changes in intracellular H₂O₂ levels. We reasoned that this trappable probe should have increased sensitivity owing to a combination of increased local concentration of probe substrate retained within cells as well as a decreased rate of deprotected probe product leaking out of cells. PF6 features two visible region absorptions ($\lambda_{\text{abs}} = 460 \text{ nm}$, $\epsilon = 14,000 \text{ M}^{-1}\text{cm}^{-1}$; 370 nm , $\epsilon = 10,000 \text{ M}^{-1}\text{cm}^{-1}$) and a weak emission ($\lambda_{\text{em}} = 530 \text{ nm}$, $\Phi = 0.10$). Spectrophotometric studies confirm that PF6 responds to H₂O₂ by a turn-on fluorescence response and is selective for H₂O₂ over a host of other ROS oxidants (Fig. 1a,b). Kinetics measurements of the H₂O₂-mediated boronate deprotection were performed under pseudo-first-order conditions (5 μM dye, 10 mM H₂O₂), giving an observed rate constant of $k = 3.3(1) \times 10^{-3} \text{ s}^{-1}$.

Validation of PF6 for molecular imaging in cell culture

With data characterizing the properties and H₂O₂-induced turn-on response of PF6 *in vitro*, we sought to evaluate its utility for molecular imaging in cell culture model systems. First, we assayed whether the AM ester cage groups were sufficient to increase retention of the probe within living cells. We utilized the boronate-based H₂O₂ probe Peroxy Green 1 (PG1), which is sensitive to signaling levels of H₂O₂ but does not possess esterase-cleavable groups, as a benchmark for these studies. PG1 and PF6 utilize the same excitation and emission wavelengths and exhibit similar emission characteristics, allowing for direct comparison of the uptake and retention these probes in cell culture by scanning confocal microscopy. After loading HeLa cells with either PG1 or PF6-AM, excess dye was thoroughly washed away. The cells were then imaged immediately after washing and visualized again after 10, 30, and 60 minutes (Fig. 1c,d). Cells loaded with PG1 show modest intracellular fluorescence immediately after washing, but the signal drops off markedly by the 10-minute time point. In contrast, cells loaded with PF6-AM exhibit intracellular fluorescence immediately after washing that is approximately twice as bright as PG1-loaded cells and maintain this emission intensity throughout the time course of the measurements. A similar trend is observed in analogous experiments using HEK 293 cells (Supplementary Fig. 3).

We next established whether this increased cellular uptake and retention would permit PF6 to detect low levels of H₂O₂ in live samples. HeLa cells were loaded with PF6-AM and then stimulated with either 10 μM H₂O₂ or carrier for 30 minutes (Fig. 1e,f). Cells treated with H₂O₂ show increased intracellular fluorescence compared to control samples, even at this relatively low level of exogenously added H₂O₂. Similar results are seen in HEK 293 cells (Supplementary Fig. 3). A drawback to this approach is the probe is not retained after fixation, making it incompatible with immunostaining in fixed cell and tissue samples. Future synthetic directions include enhancing the photostability of these dyes, adding functional groups that allow for maintenance of the probe upon fixation, and expanding the color palette of trappable H₂O₂ probes for multicolor imaging experiments. Nevertheless, these experiments confirm that PF6 is a selective and sensitive reporter for intracellular H₂O₂ in live cells and further validate the strategy of increased cellular uptake and retention as a general method for increasing the sensitivity of small-molecule fluorescent probes. In this context, PF6 adds a H₂O₂-specific fluorescent probe with selectivity and sensitivity to signaling levels of this oxygen metabolite to the arsenal of currently available ROS probes, including those for general oxidants⁴⁴ and superoxide^{35,45}.

PF6 reveals that AHPs produce H₂O₂ upon FGF stimulation

After validation of PF6 in model systems, we sought to apply this new tool to the study of AHP cells. To this end, AHPs were isolated from the hippocampi of 6-week-old female Fisher 344 rats as previously described²⁵. After growth factor withdrawal, AHPs were loaded with PF6-AM and treated with either FGF-2 mitogen or carrier. Cells stimulated with FGF-2 show increased intracellular fluorescence compared to unstimulated control AHPs as shown by PF6 imaging (Fig. 2, Supplementary Fig. 7). Toxicity studies demonstrate that PF6-AM is non-toxic at the concentration utilized in this study (Supplementary Figs. 4 and 5). When coupled with the *in vitro* selectivity characterization of PF6, these data indicate

that FGF-2 induces the endogenous production of H₂O₂ in AHPs. Furthermore, these data illustrate the utility of this new chemical tool for detecting changes in low levels of H₂O₂ in live-cell settings. Intrigued at that finding that AHPs, an essential cell population of the central nervous system from development throughout adult life, produce a compound known to have potential toxic consequences in the brain⁴⁶, we next turned our attention to elucidating potential roles for H₂O₂ in physiological (rather than pathological) processes of these cells.

H₂O₂ is required for growth signaling in AHPs

With molecular imaging data establishing that AHPs produce H₂O₂ upon mitogen stimulation, we then probed whether FGF-2-induced H₂O₂ generation could influence downstream cell signaling cascades. In this regard, an intriguing relationship has emerged between endogenous H₂O₂ production and PI3-kinase-dependent (PI3K) activation of the kinase Akt, a signaling pathway that has several potentially redox-regulated components. For example, previous studies have demonstrated that PTEN, a phosphatase that opposes forward PI3K signaling, contains a catalytic active site residue Cys-124 that is reversibly oxidized by H₂O₂ to form a disulfide with Cys-71. This oxidative redox switch turns off the activity of the phosphatase, allowing the PI3K/Akt signaling cascade to propagate forward; re-reduction of this disulfide to the corresponding thiols restores PTEN phosphatase activity, resetting the cycle.⁴⁷ The PI3K-dependent activation of Akt is critical for the growth and proliferation of AHPs, as previous studies using either pharmacological inhibition of Akt or the expression of a dominant negative Akt inhibited their proliferation.⁴⁸ Accordingly, we first investigated the effects of exogenous H₂O₂ addition to AHPs by monitoring the phosphorylation status of Akt. Toxicity studies demonstrate that AHPs can withstand H₂O₂ to surprisingly high concentrations (Supplementary Fig. 6). Treatment of AHPs with H₂O₂ in the absence of FGF-2 stimulation is sufficient to trigger a marked dose-dependent increase in phospho-Akt, without increasing the phosphorylation status of another major signaling hub, the MAP kinase ERK1/2 (Fig. 3a, Supplementary Fig. 8). Previous work has shown that pharmacological inhibition of the ERK1/2 MAP kinase pathway does not strongly affect AHP proliferation.⁴⁸

We then probed the role of endogenously produced H₂O₂ on the phosphorylation status of Akt. FGF-2 stimulation of AHPs triggers a time dependent increase in the phosphorylation of Akt compared to control samples. In contrast, cells expressing Catalase, an enzyme that quickly destroys H₂O₂, have diminished FGF-2-induced phosphorylation of Akt (Fig. 3b) and produce less detectable H₂O₂ by PF6-AM imaging (Fig. 2b, Supplementary Fig. 7). Additionally, pretreatment with the general antioxidant *N*-acetylcysteine (NAC), which will quench H₂O₂, or the flavin/Nox inhibitor diphenyliodonium (DPI), which inhibits the majority of potential intracellular sources of H₂O₂, both block the FGF-2-induced phosphorylation of Akt, as well as affect the phosphorylation of ERK1/2 to a lesser extent (Fig. 3c). To confirm that DPI at this concentration is concomitantly blocking the H₂O₂ signal and Akt phosphorylation, pretreatment of PF6-AM-loaded AHPs with DPI was shown to abolish FGF-2-induced H₂O₂ production (Fig. 2a, Supplementary Fig. 7). These experiments demonstrate that AHPs utilize redox chemistry to modulate this growth-signaling kinase pathway. We then attempted to identify potential targets of the H₂O₂ along

the Akt pathway. We utilized a methodology for assaying the oxidation status of PTEN that relies on differences in gel mobility between the oxidized, disulfide form and the reduced form of the protein⁴⁹ to demonstrate that FGF stimulation does indeed produce a small but detectable amount of oxidized PTEN (Supplementary Fig. 9). However, this approach toward assaying the oxidation state of PTEN is not very sensitive or consistent in this system, which is why we continued to monitor Akt phosphorylation, a much more reliable readout of redox signaling.

Nox2 is the source of H₂O₂-mediated signaling in AHPs

We next elucidated the molecular source of the redox signal within the AHPs. Given the vast expression of Nox2 in the CNS²¹, we looked to this protein as a potential redox modulator in AHPs. Both RT-PCR (Fig. 3d) and western blot analysis using two separate Nox2 antibodies, a rabbit and a mouse (Fig. 3e), confirm its presence in AHPs. Both antibodies show a band at the same molecular weight that corresponds to the approximate molecular weight of Nox2 (c.a. 65 kDa) and whose intensity selectively decreases upon genetic manipulation with Nox2-targeted shRNA. The mouse antibody has a nonspecific band slightly below the Nox2 band that does not change upon treatment with Nox2 shRNA, which can serve as a loading control. We utilized genetic manipulation of Nox2 to elucidate the contributions of this protein to Akt proliferation/signaling pathways as well as the fluorescent signal measured by PF6-AM. AHPs transfected with Nox2-targeted shRNA exhibit decreased Nox2 levels and show a concomitant marked decrease in FGF-2-induced phosphorylation of Akt compared to control cells transfected with an empty vector (Fig. 3f). As was observed for chemical inhibition by NAC or DPI, the ERK1/2 pathway in AHPs also appears to be affected by the lack of Nox2. AHPs transfected with Nox2-targeted shRNA also show less H₂O₂ production in response to FGF-2 stimulation (Fig. 2c, Supplementary Fig. 7). As a further validation of the shRNA knockdown experiments, we designed and tested another shRNA construct to target an alternative member of the Nox family, Nox3. Again, Nox2-shRNA transfected cells show reduced levels of Nox2 compared to Nox3-shRNA transfected cells and concomitantly exhibit a decreased response to FGF-2-induced phospho-Akt production (Fig. 3g), confirming the specific effects of the Nox2 shRNA. Taken together, these data demonstrate that Nox2-generated H₂O₂ contributes to the regulation of growth-signaling pathways within the AHPs.

Nox2 is required for normal AHP proliferation *in vitro*

With data establishing that intracellular redox changes affect signaling at the protein level, we then sought to determine whether decreased redox signaling would also manifest similar results in functional assays. We therefore investigated the effects of diminished redox signaling on AHP proliferation in the presence of FGF-2. First, 5-day *in vitro* proliferation experiments were performed in the presence of varying levels of DPI. We observed a dose-dependent decrease in growth rate with DPI inhibition, with concentrations as low as 50 nM having an inhibitory effect (Fig. 4a). As DPI is relatively non-specific and will block all flavin-containing sources of ROS, we sought to elucidate the role of Nox2 specifically. We therefore transfected AHPs with shRNA constructs targeting Nox2 or the empty vector. In agreement with the chemical inhibition experiments and western blot analysis, the Nox2 shRNA transfected cells show a diminished proliferation rate compared to AHPs containing

the empty vector (Fig. 4b), or compared to cells expressing Nox3 shRNA as a control (Fig. 4c). Taken together, these data indicate that FGF-2 signaling involves the production of H₂O₂ through the activation of Nox2, which influences signaling through Akt and ultimately the downstream phenotype of growth rate.

Nox2 is required for normal AHP function *in vivo*

We then sought to extend these *in vitro* findings to an *in vivo* system. To this end, we performed bromodeoxyuridine (BrdU) incorporation experiments in Nox2 knockout (Nox2^{-/-}) mice and CL57BL/6J control mice. BrdU incorporates into the genome of dividing cells, which can then be detected by immunohistochemistry post fixation along with stem cell or neuronal markers. Therefore, cells that stain for both BrdU as well as a stem cell marker are AHPs that proliferated during the course of the injections. Mice were injected with BrdU daily for 7 days and perfused 24 h after the final injection. Immunohistochemical assessments of the dentate gyri from Nox2^{-/-} and control mice show no morphological abnormalities (Fig. 4d,e), suggesting that the dentate gyrus develops normally in the Nox2^{-/-} mice. However, quantification of the proliferating AHP populations based on colocalization of BrdU and Sox2, a stem cell marker,⁵⁰ reveals a marked decrease in the number of proliferating AHPs in the Nox2^{-/-} mice (Fig. 4f-h), establishing that Nox2 contributes to the normal proliferation of AHPs *in vivo*.

Finally, we assayed the effects of Nox2 deficiency on adult neurogenesis *in vivo*. For these experiments mice were injected with BrdU daily for 7 days and were then perfused 28 days after the final injection. The brains were then analyzed for cells that stain for both BrdU and NeuN, a neuronal marker, which would indicate neurons that had differentiated from AHPs within the time course of the experiment. Quantification of the colocalization of BrdU and NeuN reveals a reduction in the number of newborn neurons in the Nox2^{-/-} mice (Fig. 4i-k), establishing that Nox2 also contributes to adult neurogenesis *in vivo*.

Discussion

H₂O₂ is emerging as a newly recognized messenger for cell signaling, and a major source of peroxide produced through stimulation of various cell surface receptors is the Nox family of proteins^{5,9,10,26}. These ROS-generating enzymes are classically associated with phagocytic cells during immune responses, where they are used to combat pathogens by attacking them with controlled oxidative bursts. More recent results have revealed the widespread distribution of Nox complexes in non-phagocytic cell types throughout the body⁵, presaging that H₂O₂ generation is a necessary component for physiological purposes; however, many aspects of how and why this small-molecule oxidant is required and used for the benefit of living organisms remain elusive. To address these questions, we developed a novel H₂O₂-specific fluorescent probe, PF6, and applied this new chemical tool to help demonstrate that AHPs, an essential population of cells that proliferate in the brain from development throughout adult life, respond to growth conditions by producing H₂O₂. Through a combination of imaging, pharmacological, and genetic experiments, we reveal that Nox2 and H₂O₂ are important for maintaining normal signaling and proliferation of AHPs *in vitro*. Moreover, we show that mice lacking functional Nox2 have a decreased

number of proliferating neural stem cells and less adult neurogenesis in the hippocampus, which establishes that H₂O₂-mediated redox signaling is essential on the whole organism scale.

The collective data provide a molecular model for the cognitive deficits observed in mice and humans lacking the ROS-generating Nox2 enzyme (Fig. 5) and establish that ROS are not exclusively detrimental to brain tissue in the context of seizures, stroke, and neurodegeneration. Since various isoforms of the Nox family are present throughout the brain and CNS⁴, there are likely many other beneficial roles for these ROS-producing proteins in this system. Indeed, the *in vivo* effects observed in the Nox2 knockout mice could also be influenced by a lack of Nox2 in other cell types within brain. In a broader sense, our findings show that controlled ROS production and signaling can be used as a strategy for maintaining proliferation of essential cell populations in the body. Finally, these results suggest caution when applying antioxidant therapeutics in a non-specific fashion, as ROS production can be a necessary component for the fitness of a given system.

Methods

6-Carboxyfluorescein monotriflate (2)

6-Carboxyfluorescein (512 mg, 1.36 mmol) was added to a vial and dissolved in 15 mL of 2:1 acetonitrile/DMF. Diisopropylethylamine (2.2 mL, 13.3 mmol) was then added and the reaction stirred for 10 min. *N*-Phenyl bis(trifluoromethanesulfonamide) (487 mg, 1.36 mmol) was then added and the reaction was stirred overnight at room temperature. The reaction mixture was then dried under reduced pressure. Purification by column chromatography (19:1 dichloromethane/methanol) afforded compound **2** as a yellow oil (412 mg, 60% yield). ¹H NMR (CDCl₃/10% CD₃OD, 400 MHz): δ 8.26 (1H, d, *J* = 8.0 Hz), 8.02 (1H, d, *J* = 8.2 Hz), 7.77 (1H, s), 7.19 (1H, d, *J* = 2.4 Hz), 6.90 (1H, dd, *J* = 2.4, 8.8 Hz), 6.82 (1H, d, *J* = 8.8 Hz), 6.76 (1H, d, *J* = 2.4 Hz), 6.59 (1H, dd, *J* = 2.4, 8.8 Hz), 6.54 (1H, d, *J* = 8.8 Hz). ¹³C NMR (CDCl₃/10% CD₃OD, 100 MHz): δ 168.6, 159.8, 152.5, 152.1, 151.8, 150.0, 138.4, 131.5, 130.0, 129.1, 128.9, 125.3, 125.1, 119.2, 116.5, 113.4, 110.5, 108.5, 103.0, 82.5. ¹⁹F NMR (CDCl₃/10% CD₃OD, 376.5 MHz): δ -71.97. HR-FABMS: calculated for [M⁺] 509.0149, found 509.0158.

PF6/PF6-AM (3/4)

Compound **2** (412 mg, 0.81 mmol), Pd(OAc)₂ (55 mg, 0.081 mmol), Bis(pinacolato)diboron (308 mg, 1.22 mmol), Cyclohexyl JohnPhos (114 mg, 0.32 mmol), diisopropylethylamine (594 mg, 4.63 mmol), and 5 mL of dioxane were added to a vial in an inert atmosphere glove box and the reaction was stirred overnight at room temperature. The vial was then brought out of the glove box and the contents were evaporated to dryness. Purification by column chromatography (19:1 dichloromethane/methanol) furnished **PF6** as a yellow solid (317 mg, 80% yield). ¹H NMR (CDCl₃/5% CD₃OD, 400 MHz): δ 8.26 (1H, d, *J* = 8.0 Hz), 8.06 (1H, d, *J* = 8.0 Hz), 7.78 (1H, s), 7.71 (1H, s), 7.39 (1H, d, *J* = 8.0 Hz), 6.72-6.76 (2H, m), 6.58 (1H, d, *J* = 8.8 Hz), 6.53 (1H, dd, *J* = 2.4, 8.8 Hz), 1.32 (12H, s). ¹³C NMR (CDCl₃/10% CD₃OD, 100 MHz): δ 169.1, 167.5, 159.1, 153.5, 152.3, 150.7, 136.9, 131.3, 129.7, 129.2, 129.0, 127.1, 125.5, 125.1, 123.6, 120.7, 112.6, 109.2, 103.1, 20.7. HR-

FABMS: calculated for $[M^+]$ 487.1559, found 487.1567. **PF6** (40 mg, 0.08 mmol), bromomethyl acetate (51 mg, 0.33 mmol), diisopropylethylamine (32 mg, 0.25 mmol), and 1 mL of DMF added to a vial and stirred at room temperature overnight. The reaction mixture was then extracted into dichloromethane, washed three times with water, washed once with brine, dried over magnesium sulfate, and dried under reduced pressure. Purification by column chromatography (7:3 ethyl acetate/hexanes) delivered **PF6-AM** as a white solid (11 mg, 22% yield). $^1\text{H NMR}$ ($(\text{CD}_3)_2\text{O}$, 500 MHz): δ 7.99-8.06 (1H, m), 7.81 (1H, t, $J = 6.0$ Hz), 7.72-7.79 (1H, m), 7.66 (1H, s), 7.43-7.50 (1H, m), 7.26-7.31 (1H, m), 6.97-7.10 (1H, m), 6.87-6.95 (1H, m), 6.81-6.88 (1H, m), 5.30-6.00 (4H, m), 2.01-2.11 (6H, m), 1.34 (12H, m). HR-FABMS: calculated for $[M^+]$ 631.1981, found 631.1979.

Cell Culture

AHPs were cultured on tissue culture polystyrene coated with poly-ornithine and 5 $\mu\text{g/mL}$ of laminin (Invitrogen) and grown in Dulbecco's modified Eagle medium (DMEM)/F-12 (1:1) high-glucose medium (Invitrogen) containing N-2 supplement (Invitrogen) and 20 ng/mL recombinant human FGF-2 (Peprotech). For FGF starvation, AHPs were washed once with (DMEM)/F-12 (1:1) high-glucose medium, and then placed in (DMEM)/F-12 (1:1) high-glucose medium without FGF for 12-16 hours.

AHP Fluorescence Imaging Experiments

Confocal fluorescence imaging studies on AHPs were performed with a Zeiss LSM510 NLO Axiovert 200 laser scanning inverted microscope and a 40 \times oil-immersion objective lens. Excitation of PF6-AM-loaded AHPs at 488 nm was carried out with an Ar laser and emission was collected using a 500-550 nm filter set. AHPs were incubated with 5 μM PF6-AM in DMEM/F12 + N-2 for 30 minutes at 37 $^\circ\text{C}$. The cells were then washed with fresh DMEM/F12 + N-2 twice. The cells were then incubated in DMEM/F12 + N-2 either with or without 20 ng/mL FGF-2 for 30 minutes, then imaged. For the DPI inhibited cells, 5 μM DPI was included in the DMEM/F12 + N-2 media for all incubations. Image analysis was performed in ImageJ (Wayne Rasband, NIH) with at least 10 cells counted per field in 4 separate fields for each condition.

Supplementary Material

Refer to Web version on PubMed Central for supplementary material.

Acknowledgments

We thank the Packard and Sloan Foundations (C.J.C.), the UC Berkeley Hellman Faculty Fund (C.J.C.), Amgen, Astra Zeneca, and Novartis (C.J.C.), and the National Institutes of Health (GM 79465 to C.J.C. and EB 007295 to D.V.S.) for providing funding for this work. C.J.C. is an Investigator with the Howard Hughes Medical Institute. B.C.D. was partially supported by a Chemical Biology Training Grant from the NIH (T32 GM066698). J.P. was partially supported by a training grant fellowship from the California Institute for Regenerative Medicine (T1-00007). We thank Prof. Mark Quinn for generous donation of Nox2 antibodies and Prof. Tsukasa Kawahara for helpful advice.

References

1. Floyd RA. Oxidative damage to behavior during aging. *Science*. 1991; 254:1597–1597. [PubMed: 1684251]
2. Harman D. The aging process. *Proc Natl Acad Sci USA*. 1981; 78:7124–7128. [PubMed: 6947277]
3. Andersen JK. Oxidative stress in neurodegeneration: cause or consequence? *Nature Med*. 2004; 10:S18–25. [PubMed: 15298006]
4. Bedard K, Krause KH. The NOX family of ROS-generating NADPH oxidases: physiology and pathophysiology. *Physiol Rev*. 2007; 87:245–313. [PubMed: 17237347]
5. Lambeth JD. NOX enzymes and the biology of reactive oxygen. *Nat Rev Immunol*. 2004; 4:181–189. [PubMed: 15039755]
6. Geiszt M, Kopp JB, Várnai P, Leto TL. Identification of Renox, an NAD(P)H oxidase in kidney. *Proc Natl Acad Sci USA*. 2000; 97:8010–8014. [PubMed: 10869423]
7. Suh YA, et al. Cell transformation by the superoxide-generating oxidase Mox1. *Nature*. 1999; 401:79–82. [PubMed: 10485709]
8. Sundaresan M, Yu ZX, Ferrans VJ, Irani K, Finkel T. Requirement for generation of H₂O₂ for platelet-derived growth factor signal transduction. *Science*. 1995; 270:296–299. [PubMed: 7569979]
9. Rhee SG. H₂O₂, a necessary evil for cell signaling. *Science*. 2006; 312:1882–1883. [PubMed: 16809515]
10. D'Autreaux B, Toledano MB. ROS as signalling molecules: mechanisms that generate specificity in ROS homeostasis. *Nat Rev Mol Cell Biol*. 2007; 8:813–824. [PubMed: 17848967]
11. Poole LB, Nelson KJ. Discovering mechanisms of signaling-mediated cysteine oxidation. *Curr Opin Chem Biol*. 2008; 12:18–24. [PubMed: 18282483]
12. Woo H, et al. Inactivation of Peroxiredoxin I by phosphorylation allows localized H₂O₂ accumulation for cell signaling. *Cell*. 2010; 140:517–528. [PubMed: 20178744]
13. Niethammer P, Grabher C, Look AT, Mitchison TJ. A tissue-scale gradient of hydrogen peroxide mediates rapid wound detection in zebrafish. *Nature*. 2009; 459:996–999. [PubMed: 19494811]
14. Paulsen CE, Carroll KS. Orchestrating Redox Signaling Networks through Regulatory Cysteine Switches. *ACS Chem Biol*. 2010; 5:47–62. [PubMed: 19957967]
15. Miller EW, Dickinson BC, Chang CJ. Aquaporin-3 mediates hydrogen peroxide uptake to regulate downstream intracellular signaling. *Proc Natl Acad Sci USA*. 2010; 107:15681–15686. [PubMed: 20724658]
16. Walder CE, et al. Ischemic stroke injury is reduced in mice lacking a functional NADPH oxidase. *Stroke*. 1997; 28:2252. [PubMed: 9368573]
17. Park L, Anrather J, Girouard H, Zhou P, Iadecola C. Nox2-derived reactive oxygen species mediate neurovascular dysregulation in the aging mouse brain. *J Cereb Blood Flow Metab*. 2007; 27:1908–1918. [PubMed: 17429347]
18. Behrens MM, et al. Ketamine-induced loss of phenotype of fast-spiking interneurons is mediated by NADPH-oxidase. *Science*. 2007; 318:1645–1647. [PubMed: 18063801]
19. Park L, et al. Nox2-derived radicals contribute to neurovascular and behavioral dysfunction in mice overexpressing the amyloid precursor protein. *Proc Natl Acad Sci USA*. 2008; 105:1347–1352. [PubMed: 18202172]
20. Zhang WEI, et al. Neuroprotective effect of dextromethorphan in the MPTP Parkinson's disease model: role of NADPH oxidase. *FASEB J*. 2004; 18:589–591. [PubMed: 14734632]
21. Sorce S, Krause KH. NOX enzymes in the central nervous system: from signaling to disease. *Antioxid Redox Signal*. 2009; 11:2481–2503. [PubMed: 19309263]
22. Pao M, et al. Cognitive function in patients with Chronic Granulomatous Disease: a preliminary report. *Psychosomatics*. 2004; 45:230–234. [PubMed: 15123849]
23. Kishida KT, et al. Synaptic plasticity deficits and mild memory impairments in mouse models of chronic granulomatous disease. *Mol Cell Biol*. 2006; 26:5908–5920. [PubMed: 16847341]
24. Zhao C, Deng W, Gage FH. Mechanisms and functional implications of adult neurogenesis. *Cell*. 2008; 132:645–660. [PubMed: 18295581]

25. Palmer TD, Markakis EA, Willhoite AR, Safar F, Gage FH. Fibroblast Growth Factor-2 Activates a Latent Neurogenic Program in Neural Stem Cells from Diverse Regions of the Adult CNS. *J Neurosci*. 1999; 19:8487–8497. [PubMed: 10493749]
26. Winterbourn CC. Reconciling the chemistry and biology of reactive oxygen species. *Nat Chem Biol*. 2008; 4:278–286. [PubMed: 18421291]
27. Barnham KJ, Masters CL, Bush AI. Neurodegenerative diseases and oxidative stress. *Nat Rev Drug Discov*. 2004; 3:205–214. [PubMed: 15031734]
28. Miller EW, Chang CJ. Fluorescent probes for nitric oxide and hydrogen peroxide in cell signaling. *Curr Opin Chem Biol*. 2007; 11:620–625. [PubMed: 17967434]
29. Chang MCY, Pralle A, Isacoff EY, Chang CJ. A selective, cell-permeable optical probe for hydrogen peroxide in living cells. *J Am Chem Soc*. 2004; 126:15392–15393. [PubMed: 15563161]
30. Miller EW, Albers AE, Pralle A, Isacoff EY, Chang CJ. Boronate-based fluorescent probes for imaging cellular hydrogen peroxide. *J Am Chem Soc*. 2005; 127:16652–16659. [PubMed: 16305254]
31. Albers AE, Okreglak VS, Chang CJ. A FRET-based approach to ratiometric fluorescence detection of hydrogen peroxide. *J Am Chem Soc*. 2006; 128:9640–9641. [PubMed: 16866512]
32. Albers AE, Dickinson BC, Miller EW, Chang CJ. A red-emitting naphthofluorescein-based fluorescent probe for selective detection of hydrogen peroxide in living cells. *Bioorg Med Chem Lett*. 2008; 18:5948–5950. [PubMed: 18762422]
33. Srikun D, Albers AE, Nam CI, Ivarone AT, Chang CJ. Organelle-Targetable Fluorescent Probes for Imaging Hydrogen Peroxide in Living Cells via SNAP-Tag Protein Labeling. *J Am Chem Soc*. 2010; 132:4455–4465. [PubMed: 20201528]
34. Dickinson BC, Chang CJ. A targetable fluorescent probe for imaging hydrogen peroxide in the mitochondria of living cells. *J Am Chem Soc*. 2008; 130:9638–9639. [PubMed: 18605728]
35. Dickinson BC, Srikun D, Chang CJ. Mitochondrial-targeted fluorescent probes for reactive oxygen species. *Curr Opin Chem Biol*. 2010; 14:50–56. [PubMed: 19910238]
36. Srikun D, Miller EW, Domaille DW, Chang CJ. An ICT-based approach to ratiometric fluorescence imaging of hydrogen peroxide produced in living cells. *J Am Chem Soc*. 2008; 130:4596–4597. [PubMed: 18336027]
37. Miller EW, Tulyathan O, Isacoff EY, Chang CJ. Molecular imaging of hydrogen peroxide produced for cell signaling. *Nat Chem Biol*. 2007; 3:263–267. [PubMed: 17401379]
38. Dickinson BC, Huynh C, Chang CJ. A Palette of Fluorescent Probes with Varying Emission Colors for Imaging Hydrogen Peroxide Signaling in Living Cells. *J Am Chem Soc*. 2010; 132:5906–5915. [PubMed: 20361787]
39. Tsien RY. A non-disruptive technique for loading calcium buffers and indicators into cells. *Nature*. 1981; 290:527–528. [PubMed: 7219539]
40. Izumi S, Urano Y, Hanaoka K, Terai T, Nagano T. A simple and effective strategy to increase the sensitivity of fluorescence probes in living cells. *J Am Chem Soc*. 2009; 131:10189–10200. [PubMed: 19572714]
41. Pluth MD, McQuade LE, Lippard SJ. Cell-trappable fluorescent probes for nitric oxide visualization in living cells. *Org Lett*. 2010; 12:2318–2321. [PubMed: 20405852]
42. McQuade LE, Lippard SJ. Cell-Trappable Quinoline-Derivatized Fluoresceins for Selective and Reversible Biological Zn(II) Detection. *Inorg Chem*. 2010
43. McQuade LE, et al. Visualization of nitric oxide production in the mouse main olfactory bulb by a cell-trappable copper(II) fluorescent probe. *Proc Natl Acad Sci USA*. 2010; 107:8525–8530. [PubMed: 20413724]
44. Hempel SL, Buettner GR, O'Malley YQ, Wessels DA, Flaherty DM. Dihydrofluorescein diacetate is superior for detecting intracellular oxidants: comparison with 2',7'-dichlorodihydrofluorescein diacetate, 5-(and 6)-carboxy-2',7'-dichlorodihydrofluorescein diacetate, and dihydrorhodamine 123. *Free Radic Biol Med*. 1999; 27:146–159. [PubMed: 10443931]
45. Robinson KM, et al. Selective fluorescent imaging of superoxide in vivo using ethidium-based probes. *Proc Natl Acad Sci U S A*. 2006; 103:15038–15043. [PubMed: 17015830]
46. Prozorovski T, et al. Sirt1 contributes critically to the redox-dependent fate of neural progenitors. *Nat Cell Biol*. 2008; 10:385–394. [PubMed: 18344989]

47. Kwon J, et al. Reversible oxidation and inactivation of the tumor suppressor PTEN in cells stimulated with peptide growth factors. *Proc Natl Acad Sci USA*. 2004; 101:16419–16424. [PubMed: 15534200]
48. Peltier J, O'Neill A, Schaffer DV. PI3K/Akt and CREB regulate adult neural hippocampal progenitor proliferation and differentiation. *Dev Neurobiol*. 2007; 67:1348–1361. [PubMed: 17638387]
49. Lee SR, et al. Reversible inactivation of the tumor suppressor PTEN by H₂O₂. *J Biol Chem*. 2002; 277:20336–20342. [PubMed: 11916965]
50. Suh H, et al. In Vivo Fate Analysis Reveals the Multipotent and Self-Renewal Capacities of Sox2+ Neural Stem Cells in the Adult Hippocampus. *Cell Stem Cell*. 2007; 1:515–528. [PubMed: 18371391]

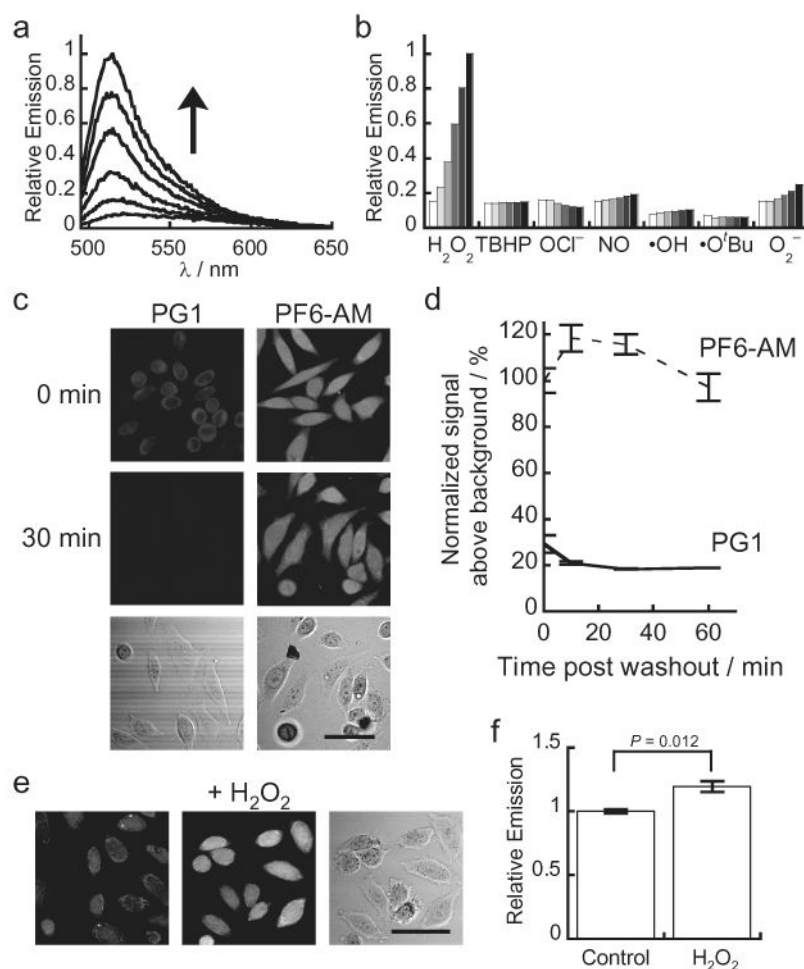


Figure 1. Spectroscopic characterization and cell culture validation of PF6-AM

(a) Fluorescence turn-on response of 5 μM PF6 at 0, 5, 15, 30, 45, and 60 minutes after the addition of 100 μM H₂O₂. (b) Fluorescence responses of 5 μM PF6 to various reactive oxygen species (ROS). Bars represent relative responses at 0, 5, 15, 30, 45, and 60 min after addition of each ROS. Data shown are for 10 mM O₂⁻ (with 10 μM Catalase), 200 μM NO, and 100 μM for all other ROS. (c) HeLa cells were loaded with either 5 μM PG1 or 5 μM PF6-AM for 15 minutes, then washed twice with DPBS and imaged at 0, 10, 30 and 60 minutes post dye washing. (d) Quantification of the experiment as conducted in (c). (e) HeLa cells were loaded with 5 μM PF6-AM for 15 minutes, stimulated with either water carrier or 10 μM H₂O₂ for 30 minutes, and imaged. (f) Quantification of the experiment as conducted in (e). Statistical analyses were performed with a two-tailed Student's *t*-test and error bars are ± s.e.m. 50 μm scale bars are shown.

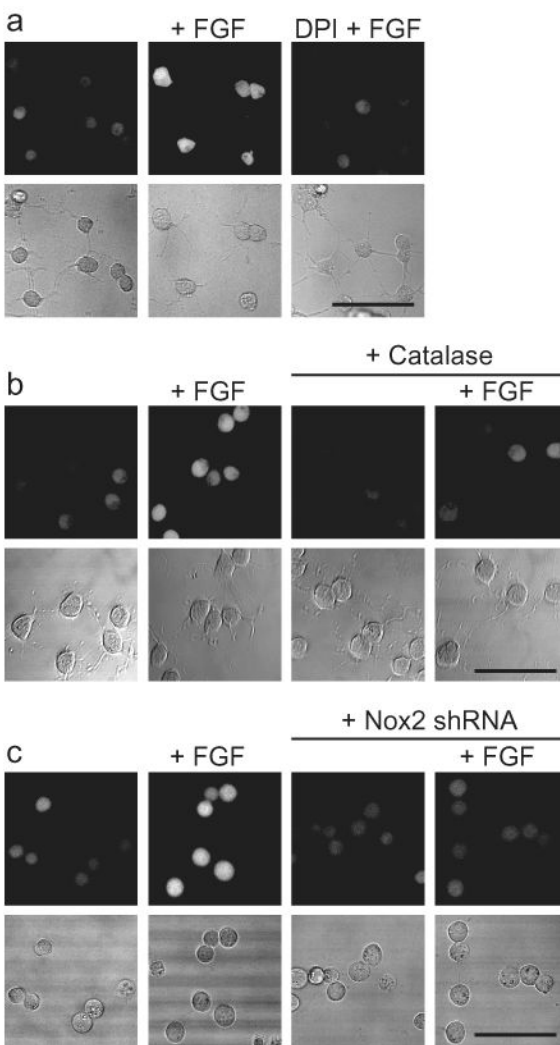


Figure 2. Application of PF6 to demonstrate that adult hippocampal stem/progenitor cells (AHPs) produce H_2O_2 upon FGF-2 stimulation

(a) After FGF-2 starvation, AHPs were loaded with 5 μ M PF6-AM for 30 minutes, stimulated with 20 ng/mL FGF-2 or media for 30 minutes, and then imaged. For DPI treatment, cells were preincubated in media containing 5 μ M DPI before FGF-2 stimulation. **(b)** AHPs were transfected with either Catalase or control vector and treated as in (a). **(c)** AHPs were transfected with either Nox2-shRNA or control vector and treated as in (a). Brightfield images are shown for each representative image with a 50 μ m scale bar.

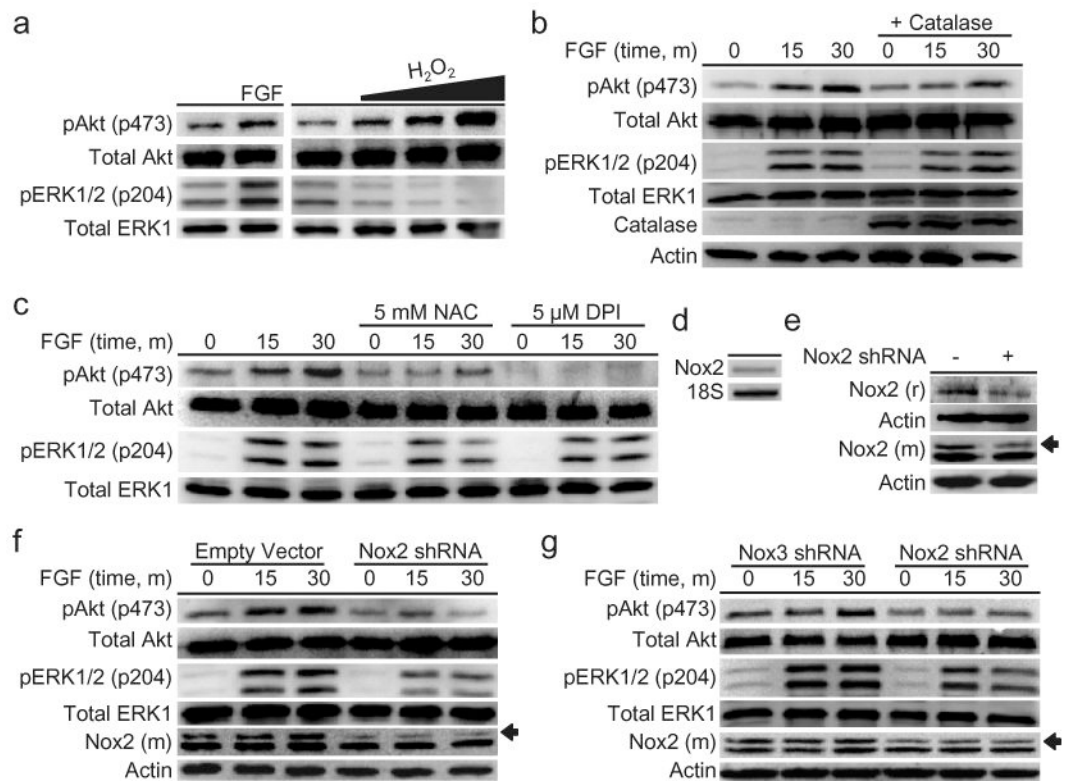


Figure 3. Cellular redox status affects AHP growth signaling

(a) After FGF-2 starvation, AHPs were stimulated with vehicle control (buffer), 20 ng/mL FGF-2, 300, 500, or 1000 μM H₂O₂ for 30 min. (b) AHPs transfected with either Catalase or a control vector. After FGF-2 starvation, AHPs were stimulated with 20 ng/mL and lysed at the given time points. (c) After FGF-2 starvation, AHPs were incubated with NAC, DPI, or vehicle control (DMSO) for 40 minutes, then stimulated with 20 ng/mL FGF-2 and lysed at the given time points. (d) Nox2 mRNA detection in AHPs measured by RT-PCR. (e) Nox2 expression of AHP whole cell extracts transfected with either Nox2 shRNA or an empty vector as measured by western blot analysis using either a mouse monoclonal (m) or a rabbit polyclonal (r) Nox2 antibody, followed by stripping and reprobing for actin as a loading control. An arrow shows the band in the Nox2 monoclonal antibody blot that matches the band in the Nox2 polyclonal blot, which corresponds to the molecular weight of Nox2. (f) AHPs transfected with either Nox2 shRNA or the empty vector. (g) AHPs transfected with either Nox2 shRNA or Nox3 shRNA. After 12 hour FGF-2 starvation, AHPs were stimulated with 20 ng/mL and lysed at the given time points. phospho-Akt, phospho-ERK, or mouse monoclonal Nox2 were measured by western blot analysis of whole cell extracts, and blots were stripped and reprobed for total protein or actin as loading controls.

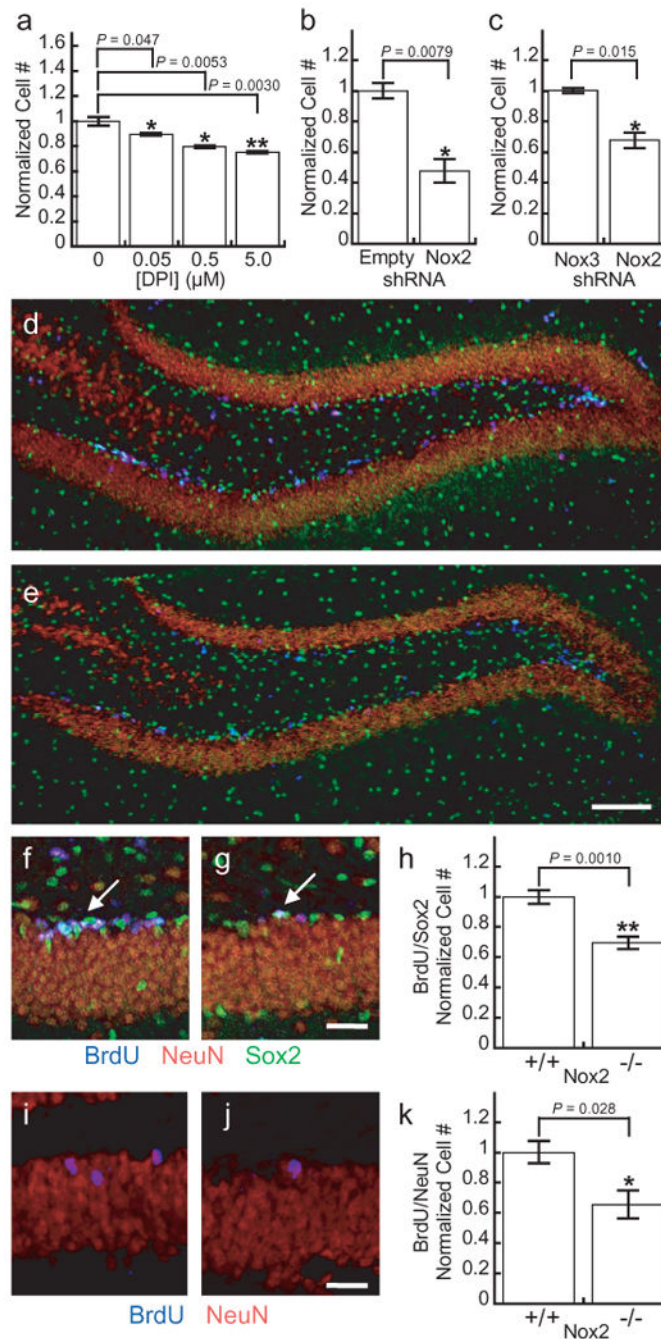


Figure 4. Nox2 is essential for normal proliferation of AHPs *in vitro* and *in vivo*

(a) 5-day growth assay of AHPs grown in the presence of FGF and varying concentrations of DPI (n = 4). (b) 5-day growth assay of AHPs transfected with either Nox2 shRNA or the empty vector and grown in the presence of FGF (n = 3). (c) 5-day growth assay of AHPs transfected with either Nox2 shRNA or Nox3 shRNA and grown in the presence of FGF (n = 3). (d) Dentate gyrus of a CL57BL/6J mouse after 7 days of BrdU injections. (e) Dentate gyrus of a Nox2^{-/-} mouse after 7 days of BrdU injections with 100 μm scale bar. (f) Example of a cluster of BrdU/Sox2 positive AHPs in a CL57BL/6J control after seven days

of BrdU injections. **(g)** Example of a single BrdU/Sox2 positive cell in a Nox2^{-/-} mouse after 7 days of BrdU injections with 20 μm scale bar. Sections stained for BrdU (blue), NeuN (red) and Sox2 (green). **(h)** Quantification of BrdU/Sox2 positive cells in either control or Nox2^{-/-} mice after 7 days of BrdU injections (n = 5). **(i)** Example of newborn neurons in a CL57BL/6J control mouse 28 days after 7 days of BrdU injections. **(j)** Example of a newborn neuron in a Nox2^{-/-} mouse 28 days after 7 days of BrdU injections with 20 μm scale bar. **(k)** Quantification of BrdU/NeuN positive cells in either control or Nox2^{-/-} mice 28 days after 7 days of BrdU injections (n = 4). For all panels data were normalized to controls and statistical analyses were performed with a two-tailed Student's *t*-test. **P* < 0.05, ***P* < 0.005 and error bars are ± s.e.m.

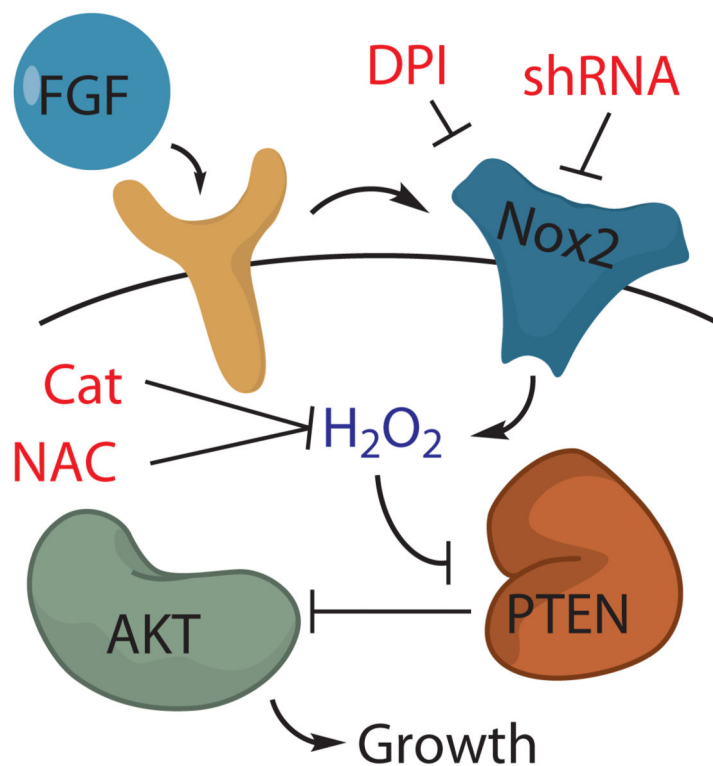
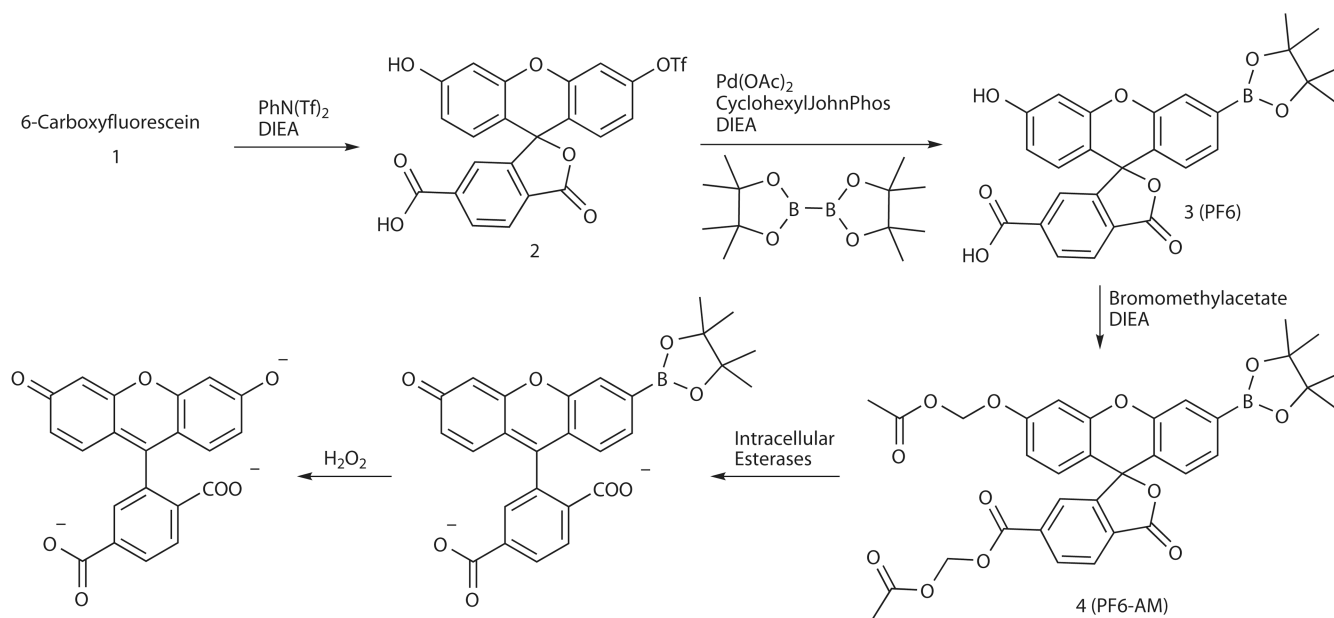


Figure 5. Model for the role of Nox2 in FGF-2 redox signaling in AHPs

The mitogen FGF-2 induces the production of H_2O_2 in AHPs, which can be blocked by either the general flavin inhibitor DPI, the antioxidant NAC, the expression of Catalase or genetic manipulation of Nox2. Nox2-generated H_2O_2 oxidizes and deactivates PTEN, which enhances signaling through Akt and manifest phenotypes in growth rates of AHPs *in vitro* and *in vivo*.



Scheme 1. Design and synthesis of Peroxyfluor-6 Acetoxymethyl Ester, PF6-AM